J Solid State Electrochem (2003) 7: 658–664
DOI 10.1007/s10008-003-0366-z

ORIGINAL PAPER

M. Lanz · C. Kormann · P. Novák

A procedure for specific charge and cycling performance measurements on $LiMn_2O_4$ spinels for lithium-ion batteries

Received: 10 February 2003 / Accepted: 10 February 2003 / Published online: 27 March 2003

Abstract A procedure for determining the specific charge and the cycling performance of lithium manganese oxide spinels ($LiMn_2O_4$) for rechargeable lithium-ion batteries has been developed. Measurements were made in two-electrode electrochemical test cells with an internal arrangement resembling that of coin cells, with either metallic lithium or a graphite composite counter electrode. Applying the procedure to various $LiMn_2O_4$ spinels with different degrees of manganese substitution, $Li_{1+y}Mn_{2-y}O_4$ ($0.05 \le y \le 0.1$), and different surface coatings, we observed an increase of the spinel cycle life with an increasing degree of manganese substitution, at the expense of a small decrease of the specific charge. The influence of the type of counter electrode on the specific charge measurements was examined. Furthermore, we investigated the influence of the temperature, 25 °C vs. 55 °C, on the specific charge and the cycling performance of the spinels with different degrees of manganese substitution. A survey of the combined effects of the counter electrode and the temperature on the specific charge measurements is given.

Keywords Cycle life · Elevated-temperature performance · $LiMn_2O_4$ spinel · Lithium-ion battery · Specific charge

Dedicated to Prof. Dr. Wolf Vielstich on the occasion of his 80th birthday in recognition of his numerous contributions to interfacial electrochemistry

M. Lanz · P. Novák (✉)
Laboratory for Electrochemistry,
Paul Scherrer Institute, 5232 Villigen, Switzerland
E-mail: petr.novak@psi.ch

C. Kormann
BASF AG, 67056 Ludwigshafen, Germany

Present address: M. Lanz
Mettler-Toledo GmbH, 8603 Schwerzenbach, Switzerland

Introduction

Numerous investigations have been made on the development and the electrochemical characterization of lithium metal oxides, e.g. $LiMn_2O_4$ spinels, for the positive electrode of rechargeable lithium-ion batteries [1, 2, 3]. Frequently in these studies, the procedures used in specific charge and cycling performance measurements or in the preparation of the electrochemical test cells are not described in full detail. It is therefore difficult to assess or compare various results. As an example, we refer to a number of recent studies on the room and elevated-temperature cycling performance of $LiMn_2O_4$ spinels [4, 5, 6, 7, 8, 9, 10, 11, 12, 13, 14, 15, 16, 17, 18, 19, 20, 21]. During our research on $LiMn_2O_4$ spinels for lithium-ion batteries, we recognized the need for a well-defined, reproducible standard procedure for specific charge and cycling performance measurements. We have developed such a procedure, and describe it in this report. We illustrate how the choice of the counter electrode, either metallic lithium or graphite, affects the specific charge measurements, and indicate a route to balance the spinel working and the graphite counter electrode for cycling performance measurements. The measurement procedure has been tested on hundreds of samples. Here, we present data on a few representative lithium manganese oxide spinels with part of the manganese ions substituted by lithium, $Li_{1+y}Mn_{2-y}O_4$ ($0.05 \le y \le 0.1$), and with different surface coatings. The results are compared with available literature data. Replacing some of the manganese in $LiMn_2O_4$ spinels with mono- or multivalent cations (e.g., Li^+, Mg^{2+}, or Zn^{2+}) was one of the important steps towards improving the room temperature cycling performance of the spinels [3, 22]. On the other hand, modifying the spinel surface with a protective encapsulation has been one of the strategies examined to improve cycling performance of $LiMn_2O_4$ spinels at elevated temperatures (~55 °C) [13, 14, 20].

Another objective of the present work was to compare the cycling performance of the spinels at 25 °C and

at 55 °C, with the aim of opening up a way to accelerated cycling tests for spinel samples.

Experimental

Spinel synthesis and physical characterization

Spinel-type lithium manganese oxides with different degrees of manganese substitution, $Li_{1+y}Mn_{2-y}O_4$ ($0.05 \le y \le 0.1$), were synthesized using a proprietary ceramic process [23]. A mixture of manganese oxide (Mn_3O_4) with a specific surface area of about 10 ± 5 m^2/g and ground lithium carbonate with a particle size of less than about 40 μm was heated for 1 h under N_2 to about 750 °C. The resulting product did not yet have a spinel structure. It was then thoroughly ground to yield a spinel precursor material. This material was oxidized in O_2 (or air) at a temperature of about 780 °C to form the spinel. Some of the spinels were coated with Li_2CO_3 or substances such as $Li_2C_2O_4$, $Y(NO_3)_3$, $Ca(NO_3)_2$, or $Ba(OH)_2$ by spray-drying an aqueous slurry of the spinel and the coating substance in a stream of hot air (200–300 °C).

The lattice constants of the spinels were determined at room temperature by powder X-ray diffraction in a Siemens D5000 diffractometer. The spinels were mixed with a small amount of SiO_2 powder as an internal standard. The lithium content of the spinels was calculated by linear interpolation of the lattice constants of 8.248 Å for $Li_{1.00}Mn_{2.00}O_4$ and 8.16 Å for $Li_{1.33}Mn_{1.67}O_4$ [24, 25]. The lattice constants and the coatings of various spinels with different lithium content are given in Table 1.

Particle sizes were determined by laser scattering measurements of aqueous slurries of the spinels using instruments from Helos or Malvern. All the spinels had an average particle size of about 10–15 μm.

Scanning electron microscopy (SEM) was used to investigate the particle morphology before and after some of the cycling experiments. SEM micrographs were taken using a Zeiss DSM960 microscope. No significant change of particle morphology was detected even after several hundred cycles at room temperature. In particular, no formation of amorphous structures could be observed on the surfaces of the spinel crystals at high resolution (magnification 20,000×).

For a determination of the Brunauer-Emmett-Teller (BET) specific surface area, the spinel powders were first dried for 12 h at 140 °C. The BET specific surface area was then measured with a Ströhlein sorptometer using the single-point-difference method according to Haul and Dümbgen, and found to be about 0.7–1.0 m^2/g for the spinels investigated.

Electrochemical measurements

The working electrode was prepared as follows: 1.000 g of lithium manganese oxide spinel sample, 50 mg of graphite (TIMREX SFG 6, Timcal), 50 mg of carbon black (ENSACO 250E, M.M.M.), and 110 mg of poly(vinylidene fluoride) (SOLEF PVDF 1015, Solvay) were blended for several minutes with approximately 3.5 g of 1-methyl-2-pyrrolidone (Fluka, puriss. p.a.) with a high-speed stirrer, and sprayed with an air-brush onto a titanium current collector disk (area 1.33 cm^2). The amount of composite electrode material deposited on the current collector was about 30 mg/cm^2. This loading of the positive electrode compares well with the typical loadings (of $LiCoO_2$) used in commercial lithium-ion cells, viz. ~20–30 mg/cm^2 [26]. The porosity of the electrodes prepared with this air-brush technique was estimated to be about 70% [27], which is higher than that found in commercial lithium-ion cells (40–50% porosity [28] should be considered as an upper limit for industrial lithium-ion batteries).

As a counter electrode, either metallic lithium (Aldrich, 99.9%) or a graphite composite coated on a copper foil was used. The graphite composite counter electrode was prepared by coating a slurry of 91 wt% of graphite (TIMREX SLM 44, Timcal) and 9 wt% of poly(vinylidene fluoride) (SOLEF PVDF 1015, Solvay) with a doctor blade onto the copper foil. The amount of counter electrode composite material applied was about 10 mg/cm^2; it was carefully balanced against the amount of working electrode active material (see below).

The electrolyte used in all the experiments was ethylene carbonate (EC)/dimethyl carbonate (DMC) (1:1 w/w) with 1 M $LiPF_6$, purchased from Merck (battery electrolyte Merck LP30, Selectipur). The H_2O content was < 10 ppm as determined by Karl-Fischer titration, and the HF content was about 50 ppm. The electrolyte was stored and handled in an argon-filled glove box.

The electrochemical test cell had an internal arrangement resembling that of coin cells. It was assembled and sealed in an argon-filled glove box, after drying all parts of the cell, including the electrodes, for at least 16 h under vacuum at 120 °C. The spinel-coated working electrode, a 1 mm thick soft glass-fiber separator (type EUJ116, Hollingworth & Vose, UK) soaked with the electrolyte, and the counter electrode were pressed together with a spring (pressure ~2 kg/cm^2), and the cell was sealed with a soft polyethylene O-ring. For the measurements with a lithium counter electrode, two glass-fiber separators were used instead of just one.

In the cycling tests with a graphite counter electrode (cycling performance and specific charge measurements), a current of 50 μA per milligram of spinel (~$C/2$ charge/discharge rate) was applied, except for the first cycle (formation cycle), which was carried out with a current of 10 μA per milligram of graphite (~$C/30$ charge/discharge rate). The cell was cycled between 3.3 V and 4.3 V. When the initial/final cell voltage was reached, the voltage was kept constant until the current dropped to 10% of the initial galvanostatic current. In the cycling tests with a metallic lithium counter electrode (specific charge measurements), a current of 10 μA per milligram of spinel (~$C/10$ charge/discharge rate) was applied, and the cell was cycled between 3.3 V and 4.3 V.

Table 1 Lattice constants and coatings of lithium manganese oxide spinels for cycling measurements

Spinel ($Li_{1+y}Mn_{2-y}O_4$)	Lattice constant (Å)	Coating[a]
$Li_{1.10}Mn_{1.90}O_4$	8.221	–
$Li_{1.09}Mn_{1.91}O_4$ (a)	8.224	0.5% $Ba(OH)_2$, 1% Li_2CO_3
$Li_{1.09}Mn_{1.91}O_4$ (b)	8.224	1% Li_2CO_3
$Li_{1.07}Mn_{1.93}O_4$ (a)	8.229	0.5% $Y(NO_3)_3$, 1% Li_2CO_3
$Li_{1.07}Mn_{1.93}O_4$ (b)	8.229	0.5% $Ca(NO_3)_2$, 1% Li_2CO_3
$Li_{1.07}Mn_{1.93}O_4$ (c)	8.229	2% $Li_2C_2O_4$, 1% Li_2CO_3
$Li_{1.07}Mn_{1.93}O_4$ (d)	8.229	2% $Li_2C_2O_4$, 0.5% $Ca(NO_3)_2$, 0.5% Li_2CO_3
$Li_{1.07}Mn_{1.93}O_4$ (e)	8.230	1% Li_2CO_3
$Li_{1.05}Mn_{1.95}O_4$	8.234	–

[a]Percentage values: wt% of the coating substance used in the coating process

Results and discussion

Specific charge and cycling performance of spinels with different degrees of manganese substitution

Specific charge

The specific charge of various lithium manganese oxide spinels with different degrees of manganese substitution, $Li_{1+y}Mn_{2-y}O_4$ ($0.05 \leq y \leq 0.1$), and with different surface coatings, was investigated at 25 °C and 55 °C. The specific charge was determined from the 1st electrochemical charge/discharge cycle. Measurements were made both with a metallic lithium and with a graphite counter electrode. When using the graphite counter electrode, the amount of graphite composite applied to the counter electrode was balanced against the amount of working electrode active material (see below). The results of the experiments are listed in Table 2 (25 °C) and Table 3 (55 °C). The irreversible capacity of the 1st cycle (i.e., the irreversible specific charge) was calculated as the difference between the 1st charge capacity (i.e., the specific charge of the charging half-cycle; lithium extraction from the spinel) and the 1st discharge capacity (i.e., the specific charge of the discharging half-cycle; lithium insertion into the spinel). The listed numbers are average values of two or three measurements each.

Figure 1 shows the specific charges (charge capacity, discharge capacity, irreversible capacity) of the 1st cycle of the lithium manganese oxide spinels at 25 °C and 55 °C; the data plotted in Fig. 1 were measured with a metallic lithium counter electrode. Linear regression lines were inserted in Fig. 1 to show the trends of the data.

Tables 2 and 3 and Fig. 1 can be discussed with respect to the degree of manganese substitution. Thus the 1st charge capacity (lithium extraction from the spinel) decreased with increasing lithium content. The 1st discharge capacity (lithium insertion into the spinel) also decreased with increasing lithium content, but this trend was weaker. As a result, the 1st irreversible capacity decreased with increasing lithium content. This variation of the 1st charge and discharge capacities has been investigated before [12, 22]. Our results are in accordance with these data, and the 1st charge capacity values are close to the theoretical capacity values of the spinels for the various compositions [22]. The compositional range of the spinels investigated in our study, i.e. $0.05 \leq y \leq 0.1$ in $Li_{1+y}Mn_{2-y}O_4$, was not as large as that reported previously [12, 22], because we focused on spinels that were possibly useful for a practical lithium-ion battery. The irreversible capacity measured in the first charge/discharge cycle of the lithium manganese oxide spinels may be attributed to the formation of a solid electrolyte interphase on the spinel electrode, the existence of which has been proven recently [29].

Cycling performance

For the determination of cycling performance, a graphite counter electrode was used exclusively, since metallic lithium exhibits poor cycleability [1]. The amount of graphite was balanced against the spinel

Table 2 Average specific charge of the 1st cycle of lithium manganese oxide spinels at 25 °C; measurements with either a metallic lithium or(numbers in parentheses) a graphite counter electrode

Spinel ($Li_{1+y}Mn_{2-y}O_4$)	Charge capacity (A h/kg)	Discharge capacity (A h/kg)	Irreversible capacity (A h/kg)
$Li_{1.10}Mn_{1.90}O_4$	116 (115)	113 (105)	3 (10)
$Li_{1.09}Mn_{1.91}O_4$ (a)	119 (117)	114 (106)	5 (11)
$Li_{1.09}Mn_{1.91}O_4$ (b)	112 (111)	107 (100)	5 (11)
$Li_{1.07}Mn_{1.93}O_4$ (a)	125 (124)	117 (110)	8 (14)
$Li_{1.07}Mn_{1.93}O_4$ (b)	122 (123)	116 (109)	6 (14)
$Li_{1.07}Mn_{1.93}O_4$ (c)	119 (120)	113 (108)	6 (12)
$Li_{1.07}Mn_{1.93}O_4$ (d)	119 (121)	113 (109)	6 (12)
$Li_{1.07}Mn_{1.93}O_4$ (e)	122 (126)	112 (110)	10 (16)
$Li_{1.05}Mn_{1.95}O_4$	126 (127)	113 (109)	13 (18)

Table 3 Average specific charge of the 1st cycle of lithium manganese oxide spinels at 55 °C; measurements with either a metallic lithium or(numbers in parentheses) a graphite counter electrode

Spinel ($Li_{1+y}Mn_{2-y}O_4$)	Charge capacity (A h/kg)	Discharge capacity (A h/kg)	Irreversible capacity (A h/kg)
$Li_{1.10}Mn_{1.90}O_4$	120 (117)	110 (101)	10 (16)
$Li_{1.09}Mn_{1.91}O_4$ (a)	128 (126)	111 (78)	17 (48)
$Li_{1.09}Mn_{1.91}O_4$ (b)	121 (117)	107 (94)	14 (23)
$Li_{1.07}Mn_{1.93}O_4$ (a)	132 (130)	111 (101)	21 (29)
$Li_{1.07}Mn_{1.93}O_4$ (b)	129 (130)	111 (102)	18 (28)
$Li_{1.07}Mn_{1.93}O_4$ (c)	130 (128)	110 (100)	20 (28)
$Li_{1.07}Mn_{1.93}O_4$ (d)	130 (131)	111 (104)	19 (27)
$Li_{1.07}Mn_{1.93}O_4$ (e)	132 (133)	109 (99)	23 (34)
$Li_{1.05}Mn_{1.95}O_4$	134 (136)	113 (100)	21 (36)

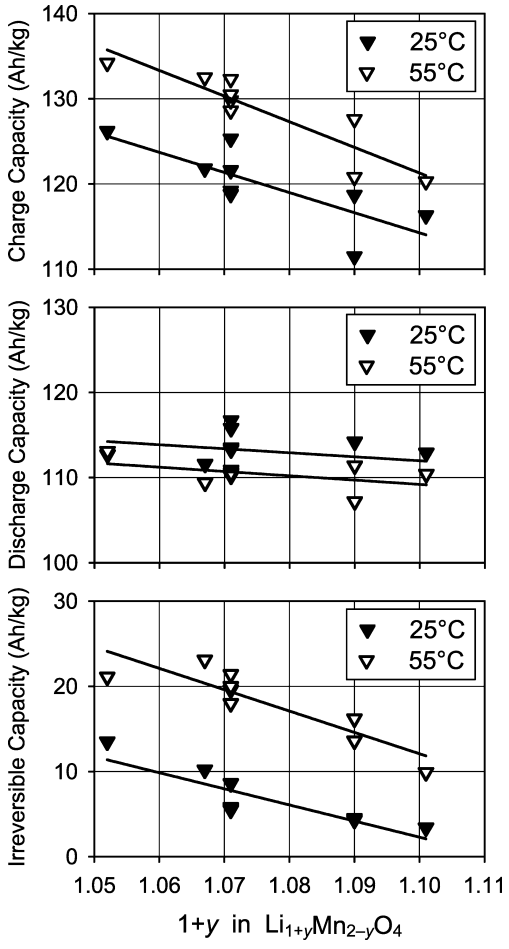

Fig. 1 Dependence of the specific charges (charge capacity, discharge capacity, and irreversible capacity) of the 1st cycle of lithium manganese oxide spinels on the lithium excess y in $Li_{1+y}Mn_{2-y}O_4$ at 25 °C and 55 °C; measurements with a metallic lithium counter electrode

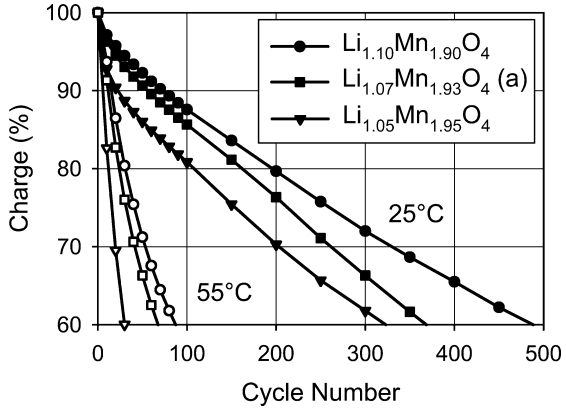

Fig. 2 Cycling performance of three different lithium manganese oxide spinels ($Li_{1+y}Mn_{2-y}O_4$) at 25 °C and 55 °C. The charge (average discharge capacity; percentage relative to the 1st discharge cycle) is plotted as a function of the cycle number

working electrode (see below). Figure 2 shows the cycling performance of three arbitrarily chosen spinels with different degrees of manganese substitution at 25 °C and 55 °C. The charge measured during the discharge cycles (i.e., the discharge capacity) is plotted versus the cycle number. For the sake of easier comparison, the discharge capacity of each spinel is plotted as a percentage of the 1st discharge cycle. The plots are average values of two or three cycling performance measurements for each spinel.

Table 4 shows the cycle life of various spinels at 25 °C and 55 °C. The cycle life is given as the number of cycles, $n_{80\%}$, that can be performed until the discharge capacity drops to 80% of its value in the 1st cycle. The numbers are average values of two or three measurements each. The last column in Table 4 is the ratio of $n_{80\%}$(25 °C) and $n_{80\%}$(55 °C); it will be discussed below. Figure 3 shows a graphical representation of the data given in Table 4. Linear regression lines are inserted in Fig. 3 to show the trends. The cycle life at 25 °C increased with increasing lithium content. The trend was similar at 55 °C. The improvement in cycle life which occurs upon partial substitution of lithium for manganese, at the expense of the specific charge of the spinel, has been discussed in the literature [3, 22]. In short, the substitution raises the average manganese-ion oxidation state to values slightly above 3.5, and thus suppresses the detrimental phase transition from cubic to tetragonal occurring in the spinel upon deep discharge ($z \approx 1$ in $Li_zMn_2O_4$) owing to the Jahn-Teller effect of the Mn^{3+} ions [3, 22].

Effect of the counter electrode

Balancing of the working electrode and the graphite counter electrode

For the measurements with a graphite counter electrode, the amount of graphite was balanced against the spinel working electrode. When the "rocking-chair" type lithium-ion cell is charged, lithium is extracted from the spinel and intercalated into the graphite. Part of the lithium extracted from the spinel in the first charging half-cycle is irreversibly consumed by the formation of a solid electrolyte interphase (SEI) on the graphite counter electrode [30, 31]. This part of lithium is no longer available for re-insertion into the spinel in the discharge cycle. Therefore, a balancing of the amount of working and counter electrode active material is a prerequisite for well-defined measurements. In the experiments described in this report, balancing of the spinel positive electrode and the graphite negative electrode for lithium insertion/extraction was based on the following considerations. The specific charge of graphite SLM 44 was found to be close to the theoretical value for the formation of LiC_6, 372 A h per kilogram of carbon [1, 32]. The specific charge of the spinel is assumed to be about 110 A h/kg. For a perfect match of charges, the mass ratio of graphite to spinel should be 1:3.38. However, a 25% excess of graphite over the spinel was chosen, in order to avoid any lithium plating on the graphite. Such lithium

Table 4 Average cycle life (80% vs. 1st discharge), expressed as the number of cycles, $n_{80\%}$, of lithium manganese oxide spinels achieved at 25 °C and 55 °C. The last column is the quotient of $n_{80\%}$(25 °C) and $n_{80\%}$(55 °C)

Spinel ($Li_{1+y}Mn_{2-y}O_4$)	$n_{80\%}$(25 °C)	$n_{80\%}$(55 °C)	$N_{80\%}$(25 °C)/ $n_{80\%}$(55 °C)
$Li_{1.10}Mn_{1.90}O_4$	196	31	6
$Li_{1.09}Mn_{1.91}O_4$ (a)	165	17	10
$Li_{1.09}Mn_{1.91}O_4$ (b)	201	22	9
$Li_{1.07}Mn_{1.93}O_4$ (a)	162	24	7
$Li_{1.07}Mn_{1.93}O_4$ (b)	146	30	5
$Li_{1.07}Mn_{1.93}O_4$ (c)	196	36	5
$Li_{1.07}Mn_{1.93}O_4$ (d)	208	30	7
$Li_{1.07}Mn_{1.93}O_4$ (e)	113	15	8
$Li_{1.05}Mn_{1.95}O_4$	108	12	9

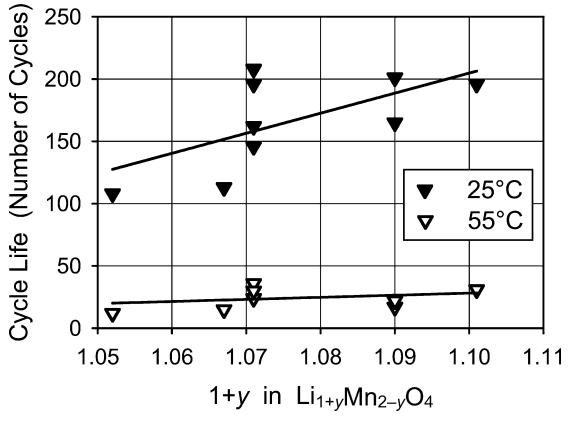

Fig. 3 Dependence of the cycle life (80% vs. 1st discharge) of lithium manganese oxide spinels on the lithium excess y in $Li_{1+y}Mn_{2-y}O_4$, at 25 °C and 55 °C; measurements with a graphite counter electrode

deposits can react with the solvent to form a SEI film and become partly electrochemically inactive; in the worst case, lithium dendrites penetrate the separator and locally short-circuit the cell [1]. Thus, a mass ratio of 1:2.7 was chosen for all experiments discussed in this report, with a mass tolerance of ±3%.

Graphite versus metallic lithium counter electrode

The specific charge measurements were made both with metallic lithium and with a graphite counter electrode. We compare these two series of measurements. The 1st charge (lithium extraction from the spinel) capacity was the same for both types of counter electrodes for the spinels within an experimental precision of about ±3% (see Tables 2 and 3). Thus, as expected, the amount of lithium that could be extracted from the spinel did not depend on the counter electrode. The 1st discharge (lithium re-insertion into the spinel) capacity, however, was smaller with a graphite counter electrode than with a metallic lithium counter electrode. Therefore, larger values were calculated for the 1st irreversible capacity when using the graphite counter electrode. This was due to the irreversible consumption of lithium in the formation of the SEI film on the graphite counter electrode. Note that the cell cut-off voltage was 3.3 V during discharge in these experiments, i.e. an over-oxidation of the graphite counter electrode was avoided. The discrepancy between discharge capacity values found with the graphite and the metallic lithium counter electrode was larger at 55 °C than at 25 °C, i.e. the irreversible consumption of lithium on the graphite counter electrode increased with increasing temperature.

The SEI formation also takes place on a metallic lithium counter electrode. In this case, however, the counter electrode provides a large excess of lithium available for re-insertion into the spinel working electrode in the discharge cycle. We conclude that it is more useful to determine the irreversible capacity of the spinels in an electrochemical cell with a metallic lithium counter electrode than with a graphite counter electrode. The issue of the loss of lithium at the counter electrode, as well as a possible interaction between the spinel working electrode and a carbon counter electrode, has been discussed before [20, 33, 34]. Amatucci et al. [20] have demonstrated good cycleability of spinels as cathode materials in plastic lithium-ion cells (PLiON) at 55 °C, using either metallic lithium or Li_4TiO_{12} as anode materials. When graphite was used as an anode material, however, higher capacity losses were observed [20]. Reimers and co-workers [33, 34] suggested that the capacity fade mechanism for lithium-ion cells with a spinel cathode at elevated temperatures involves interactions between the carbon anode and the spinel cathode. A partial decomposition of the SEI layer on the graphite was assumed, leading to soluble species reacting with the spinel on the cathode. However, in spite of the conceivable complications related to the SEI formation and dissolution on the graphite counter electrode at elevated temperature, our cycling performance measurements with a graphite counter electrode at 55 °C were well suited for assessing and comparing the elevated temperature performance of different spinels (see below).

Comparison and correlation of measurements at 25 °C and 55 °C

Specific charge

We compared the specific charges of the 1st cycle at 25 °C and 55 °C (see Tables 2 and 3 and Fig. 1). For all the spinels, the measurement of the 1st charge capacity yielded a higher value at 55 °C than at 25 °C. This was probably due to enhanced irreversible side reactions, e.g. oxidation of the electrolyte solvent [35, 36], and decomposition of the electrolyte salt $LiPF_6$ [37], which occurred in addition to lithium extraction from the spinel, and thus led to a significantly higher charge capacity at 55 °C. On the other hand, the measurement of the 1st discharge capacity yielded a slightly lower value at 55 °C than at 25 °C. This points to a capacity fading

of the spinel taking place in the first charge/discharge cycle, which was stronger at 55 °C than at 25 °C. As a consequence, the calculated 1st irreversible capacity of the spinels was higher at 55 °C than at 25 °C.

Cycling performance

In Table 4 and Fig. 3 the spinel cycle lives (80% vs. 1st discharge) at 25 °C and 55 °C are compared. Table 4 gives the ratio $n_{80\%}$(25 °C)/$n_{80\%}$(55 °C) of the number of cycles at 25 °C and the number of cycles at 55 °C. At 55 °C the capacity fading of the spinels $Li_{1+y}Mn_{2-y}O_4$ was 5–10 times higher (average factor 7.3) than at 25 °C, when related to the cycle number. The ratio $n_{80\%}$(25 °C)/$n_{80\%}$(55 °C) shows a decreasing trend with increasing lithium content, except for $Li_{1.09}Mn_{1.91}O_4$ which did not follow this trend. This means that the improvement of the cycling performance of the spinels by manganese substitution is even more pronounced at 55 °C than at 25 °C.

Surface modification of lithium manganese oxide spinels, e.g. to reduce the expected acid attack in $LiPF_6$-containing electrolytes, has been suggested as a method to improve their elevated-temperature performance [13, 14, 20]. We therefore coated a series of spinels with Li_2CO_3 and other substances (see Table 1). However, the elevated-temperature performance of the spinels was not significantly improved over that of the uncoated spinels (Fig. 3). On the contrary, the surface-coated spinels $Li_{1.09}Mn_{1.91}O_4$ (a) and (b) show an extraordinarily poor elevated-temperature cycling performance.

Influence of the cell components

Apart from the working electrode active material, a number of additional parameters influence the cycling performance measurements, e.g. the selection of cell components and the cell construction. Thus, we found somewhat different results in absolute cycle numbers in experiments using real coin cells [38], but the trends were similar. We could demonstrate with a graphite/$LiMn_2O_4$ coin cell that 60% of the charge was still available after about 1000 deep cycles [38]. However, the spinel electrode in this coin cell had retained about 79% of its initial capacity (with respect to the first discharge), according to measurements made in a test cell with a lithium counter electrode after removing the spinel electrode from the cycled coin cell. This experiment shows that only a part of the capacity fading occurring during cycling is due to the spinel electrode. Thus, care must be taken when comparing achievements discussed in the literature with one another. Some of the relevant parameters affecting the cycling performance are the composite electrode binders/additives, the electrode preparation method, the electrode thickness, its porosity, the current collector material, the type of counter electrode, the balancing between the electroactive substances of the working and counter electrode, the type of electrolyte solvent and electrolyte salt, the electrolyte-to-active-material ratio, the cell separator, the geometry of the electrochemical cell, the pressure that is exerted on the electrodes, the protection of the cell against moisture and air, and the cycling conditions (cycling rate, cut-off voltage).

Conclusions

We have developed a procedure for measurement of the specific charge and the cycling performance of lithium manganese oxide spinels at various temperatures, using an electrochemical test cell with an internal arrangement resembling that of coin cells, with either a metallic lithium or a graphite counter electrode. The procedure was applied to various spinel samples having part of the manganese ions substituted by lithium, $Li_{1+y}Mn_{2-y}O_4$ ($0.05 \le y \le 0.1$). The cycle life increased with an increasing lithium content of the spinels, at the expense of a small decrease of the 1st charge capacity. The influence of the counter electrode, graphite versus metallic lithium, on the specific charge measurements was investigated. Specific charge and cycling performance measurements at 25 °C were compared with measurements at 55 °C. The cycle life (number of cycles) of the cells was 5–10 times shorter at 55 °C than at 25 °C. This opens a way to accelerated cycling tests for spinel samples. Coating the spinels with Li_2CO_3 and other substances, in order to prevent acid attack, did not improve the elevated-temperature performance. Furthermore, we found that the cell components and cell construction affected the cycling performance measurements. We conclude that a standardized procedure is essential when comparing the cycling performance of lithium manganese oxide spinels (or other electrode materials) for lithium-ion batteries.

Acknowledgements We thank Dr. R. Imhof (PSI, now at Renata AG) and Dr. D. Häringer (PSI, now at FZ Karlsruhe) for carrying out part of the electrochemical measurements. We also thank Dr. O. Haas (PSI), Dr. P. Heilmann (BASF), Dr. H. Steininger (BASF), and Dr. G. Heil (BASF) for helpful discussions. We acknowledge financial support by EMTEC Magnetics GmbH, Germany, and by the Paul Scherrer Institute.

References

1. Winter M, Besenhard JO, Spahr ME, Novák P (1998) Adv Mater 10:725
2. Ritchie AG, Giwa CO, Lee JC, Bowles P, Gilmour A, Allan J, Rice DA, Brady F, Tsang SCE (1999) J Power Sources 80:98
3. Thackeray MM (1997) Prog Solid State Chem 25:1
4. Thackeray MM, Shao-Horn Y, Kahaian AJ, Kepler KD, Skinner E, Vaughey JT, Hackney SA (1998) Electrochem Solid-State Lett 1:7
5. Song M-Y, Ahn D-S (1998) Solid State Ionics 112:245
6. Kim M-K, Chung H-T, Um W-S, Park Y-J, Kim J-G, Kim H-G (1999) Mater Lett 39:133
7. Song D, Ikuta H, Uchida T, Wakihara M (1999) Solid State Ionics 117:151

8. Hayashi N, Ikuta H, Wakihara M (1999) J Electrochem Soc 146:1351
9. Song MY, Ahn DS, Park HR (1999) J Power Sources 83:57
10. Cho J, Thackeray MM (1999) J Electrochem Soc 146:3577
11. Huang H, Vincent CA, Bruce PG (1999) J Electrochem Soc 146:3649
12. Amatucci GG, Schmutz CN, Blyr A, Sigala C, Gozdz AS, Larcher D, Tarascon JM (1997) J Power Sources 69:11
13. Blyr A, Du Pasquier A, Amatucci G, Tarascon J-M (1997) Ionics 3:321
14. Amatucci GG, Blyr A, Sigala C, Alfonse P, Tarascon J-M (1997) Solid State Ionics 104:13
15. Inoue T, Sano M (1998) J Electrochem Soc 145:3704
16. Inoue T, Sano M (1998) Prog Batt Batt Mater 17:191
17. Du Pasquier A, Blyr A, Courjal P, Larcher D, Amatucci G, Gérand B, Tarascon J-M (1999) J Electrochem Soc 146:428
18. Huang H, Vincent CA, Bruce PG (1999) J Electrochem Soc 146:481
19. Du Pasquier A, Blyr A, Cressent A, Lenain C, Amatucci G, Tarascon J-M (1999) J Power Sources 81/82:54
20. Amatucci G, Du Pasquier A, Blyr A, Zheng T, Tarascon J-M (1999) Electrochim Acta 45:255
21. Amatucci GG, Pereira N, Zheng T, Plitz I, Tarascon J-M (1999) J Power Sources 81/82:39
22. Gummow RJ, de Kock A, Thackeray MM (1994) Solid State Ionics 69:59
23. EMTEC Magnetics GmbH, Munich, Germany (2003) Patents pending
24. Takada T, Hayakawa H, Akiba E, Izumi F, Chakoumakos BC (1997) J Power Sources 68:613
25. Endres P, Ott A, Kemmler-Sack S, Jäger A, Mayer HA, Praas H-W, Brandt K (1997) J Power Sources 69:145
26. Johnson BA, White RE (1998) J Power Sources 70:48
27. Lanz M, Kormann C, Steininger H, Heil G, Haas O, Novák P (2000) J Electrochem Soc 147:3997
28. Haas O, Deiss E, Novák P, Scheifele W, Tsukada A (1997) In: Holmes CF, Landgrebe AR (eds) Proceedings of the symposium on batteries for portable applications and electric vehicles. (Electrochemical Society proceedings vol 97-18) The Electrochemical Society, Pennington, NJ, p 451
29. Eriksson T, Gustafsson T, Thomas JO (1998) In: Surampudi S (ed) Proceedings of the symposium on lithium batteries. (Electrochemical Society proceedings vol 98-16) The Electrochemical Society, Pennington, NJ, p 315
30. Peled E (1983) In: Gabano J-P (ed) Lithium batteries. Academic Press, London, p 43
31. Ein-Eli Y (1999) Electrochem Solid-State Lett 2:212
32. Joho F, Rykart B, Blome A, Novák P, Wilhelm H, Spahr ME (2001) J Power Sources 97/98:78
33. Gee M, Reimers J, Wang Y (1998) IMLB-9 book of abstracts, Edinburgh, poster session II
34. Wang Y, Reimers J (1998) IMLB-9 book of abstracts, Edinburgh, poster session III
35. Imhof R, Novák P (1999) J Electrochem Soc 146:1702
36. Joho F, Novák P (2000) Electrochim Acta 45:3589
37. Dominey LA (1994) In: Pistoia G (ed) Lithium batteries. Elsevier, Amsterdam, p 137
38. Novák P, Joho F, Lanz M, Rykart B, Panitz J-C, Alliata D, Kötz R, Haas O (2001) J Power Sources 97/98:39